Infrared Spectra and Electronic Structure Calculations for the NUN(NN)$_{1-5}$ and NU(NN)$_{1-6}$ Complexes in Solid Argon

Lester Andrews,* Xuefeng Wang, and Yu Gong

Department of Chemistry, University of Virginia, P.O. Box 400319, Charlottesville, Virginia 22904-4319, United States, and Chemistry Department, Tongji University, Shanghai 200093, China

Bess Vlaisavljevich and Laura Gagliardi

Department of Chemistry, Supercomputing Institute, and Chemical Theory Center, University of Minnesota, Minneapolis, Minnesota 55455, United States

ⓢ *Supporting Information*

ABSTRACT: Reactions of laser-ablated U atoms with N_2 molecules in excess argon during co-deposition at 4 K gave intense NUN and weaker UN absorptions. Annealing increased progressions of new absorptions for the NUN(NN)$_{1,2,3,4,5}$ and NU(NN)$_{1,2,3,4,5,6}$ uranium nitride complexes. Small matrix shifts are observed when the secondary coordination layers around the primary NUN(NN)$_{1,2,3,4,5}$ and NU(NN)$_{1,2,3,4,5,6}$ complexes are changed from argon to nitrogen. Electronic structure and energy and frequency calculations provide support for the identification of these complexes and further characterization of the N≡U≡N and U≡N core molecules as terminal uranium nitrides with full triple bonds.
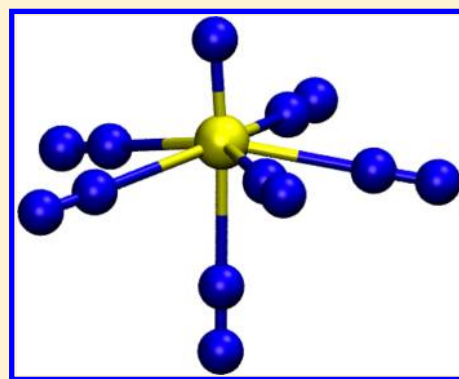
INTRODUCTION

The fact that uranium forms multiple bonds with main group elements is of considerable research interest, as attested by a current review.[1] Synthetic chemists have prepared imido (An=NX) and N−U−N molecular linkages and recently synthesized and determined the structure of ligand-stabilized terminal uranium(V) and (VI) nitride complexes.[2−4] In the solid state, three uranium nitrides are known, including UN, UN$_2$, and U$_2$N$_3$.[5] Spectroscopists have synthesized and identified the simple molecular uranium nitrides U≡N, N≡U≡N, and N≡UF$_3$ from uranium atom reactions in matrix isolation experiments, albeit on a smaller scale.[6−10] The linear N≡U≡N molecule, which is isoelectronic to the ubiquitous uranyl dication, has been observed only by matrix isolation spectroscopy.[6,7,9] In the first study, Green and Reedy sputtered a 0.5% N_2/argon mixture through a U hollow cathode and observed both UN and NUN in a solid argon matrix.[6] In later work in our laboratory, we employed laser-ablated uranium for the reaction with N_2 in argon and found an increased yield of NUN plus (NUN)(NN)$_{1,2}$ complexes, and the same reaction with pure N_2 formed even higher (NU)(NN)$_x$(NN)$_y$ complexes.[7,9]

Small molecules with multiple bonds to uranium such as N≡U=O, NH=UH$_2$, CH$_2$=UH$_2$, and U≡C have been characterized in matrix isolation experiments through reactions of laser-ablated uranium atoms.[10−14] In addition, reactions of U with N_2/H$_2$/Ar mixtures have produced the N≡U=N−H molecule, which contains both triple and double uranium–nitrogen bonds, as characterized by the infrared spectrum and theoretical computations.[15] Recently, rotationally resolved optical transitions of supersonically cooled uranium nitride (UN) have been reported, which provided a ground-state UN bond length of 1.7650(12) Å and suggested that the UN molecule is best-considered as a U^{3+}N^{3-} species in which the closed shell nitride ligand interacts with a U^{3+} ion.[16]

RESULTS AND DISCUSSION

The experimental and computational methods employed here are summarized in Supporting Information. Our first reaction of laser-ablated U atoms with N_2 trapped only the NUN product, presumably because the 12 K substrate temperature was too high for rapid quenching to isolate the quite reactive diatomic UN molecule.[7] However, weak UN matrix site absorptions were observed in subsequent NUNH work using a 4 K CsI window for argon matrix deposition.[6,8,15] The experiments were repeated for 0.5% $^{14}N_2$ samples in argon, and the infrared spectra are illustrated in Figure 1 with the new absorptions collected in Table 1. The $^{15}N_2$ counterparts, new bands using $^{14}N_2/^{14}N^{15}N/^{15}N_2$ mixtures, and the important diagnostic 14/15 isotopic frequency ratios are also listed. Note the very intense NUN absorption at 1050.9 cm^{-1} and two
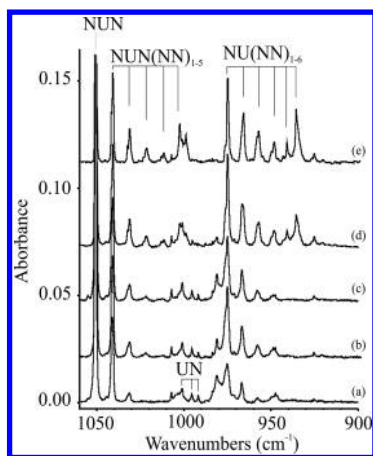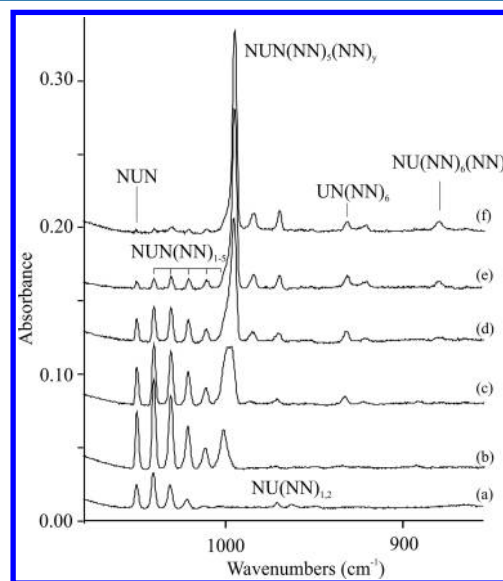
Figure 1. Infrared spectra of the major laser-ablated uranium and nitrogen reaction products. (a) U and $^{14}N_2$ (0.5%) in argon co-deposited for 60 min onto a CsI window at 4 K, (b) after annealing to 30 K, (c) after >220 nm irradiation for 20 min, (d) after annealing to 35 K, and (e) after annealing to 45 K.

saturated $NUN(NN)_5$ and $UN(NN)_6$ stoichiometries in the $NUN(NN)_{1,2,3,4,5}$ and $UN(NN)_{1,2,3,4,5,6}$ sets of complexes. The 999.0 cm^{-1} peak likely denotes the beginning of the secondary coordination layer of nitrogen molecules around $NUN(NN)_5$, which ends at 995.7 cm^{-1} in pure nitrogen.

Additional experiments were performed using higher nitrogen concentrations in argon to help determine the number of dinitrogen molecules in the primary coordination spheres around the uranium centers. Figure S1 illustrates spectra using 2.5% nitrogen, and Figure 2 shows spectra from a 10% N_2

additional bands at 1041.0 and 1031.4 cm^{-1}, which have been assigned to $NUN(NN)_{1,2}$ complexes.[7] Also, note the weaker UN bands at 1001.1, 995.6, and 991.9 cm^{-1}, as identified previously,[6] and new bands at 975.1, 965.9, 957.1, and 948.3 cm^{-1}. Subsequent annealing completed the progression of new absorptions for NN ligand complexes below the NUN and UN core absorptions, which are also listed in Table 1. Notice that both progressions decrease in intensity until the terminal bands at 1002.6 and 935.6 cm^{-1} are reached with increased intensity. This was surprising at first until it became apparent that these progressions must terminate when the primary coordination shells for each core nitride are filled. This occurs because attachment of additional NN ligands to the lower complexes forms the higher complexes at the expense of the lower complexes and leads ultimately to the absorptions for the

Figure 2. Infrared spectra of the major laser-ablated uranium and nitrogen reaction products upon co-deposition in argon onto a CsI window at 4 K. (a) U and $^{14}N_2$ (10%) in argon co-deposited for 60 min, (b) after >220 nm irradiation for 20 min, (c) after annealing to 20 K, (d) after annealing to 30 K, (e) after annealing to 35 K, and (f) after annealing to 40 K.

Table 1. Observed Frequencies (cm^{-1}) for Uranium and Nitrogen Reaction Products in Solid Argon Using 0.5% N_2 Samples[a]

$^{14}N_2$	$^{14}N_2/^{14}N^{15}N/^{15}N_2$	$^{15}N_2$	14/15 ratio	identification
1050.9	1040.7, 987.2	1019.4	1.03090	$NUN(Ar)_x$
1041.0	1031.1	1009.8	1.03090	$NUN(Ar)_4(NN)$
1031.4		1000.4	1.03099	$NUN(Ar)_3(NN)_2$
1021.6		990.8	1.03109	$NUN(Ar)_2(NN)_3$
1011.7		981.3	1.03098	$NUN(Ar)(NN)_4$
1002.6		972.4	1.03106	$NUN(NN)_5 [(Ar)_x]$
999.0		968.9	1.03107	$NUN(NN)_5 [(NN)_xAr_y$
1007.4		975.6	1.03260	unidentified UN species
1001.1	1001.1, 969.5	969.5	1.03259	$UN(Ar)_x$
995.6	995.6, 964.1	964.1	1.03267	$UN(Ar)_x$
991.9	991.9, 960.6	960.6	1.03258	$UN(Ar)_x$
981.3		950.0	1.03295	$UN(Ar)_x(NN)$ site
975.1		944.2	1.03273	$UN(Ar)_5(NN)$
965.9		935.3	1.03272	$UN(Ar)_4(NN)_2$
957.1		926.7	1.03280	$UN(Ar)_3(NN)_3$
948.3		918.4	1.03256	$UN(Ar)_2(NN)_4$
940.9		911.1	1.03271	$UN(Ar)_1(NN)_5$
935.6		906.0	1.03267	$UN(NN)_6 Ar_y$
925.3		896.2	1.03247	$UN(NN)_6 [(NN)_x]Ar_y$

[a]New frequencies listed for the $^{14}N^{15}N$ reaction product. Ar atoms are added in the identifications where they likely reside. In an argon matrix, NUN and UN are completely surrounded by argon atoms in some fashion, and these Ar atoms compete unfavorably with NN for the ligand role on annealing.

Table 2. Uranium Nitride Stretching Frequencies (cm⁻¹) and Bond Lengths (Å) for Optimized Structures of NUN(NN)$_x$ and NU(NN)$_x$ Complexes Calculated at the B3LYP Level of Theory^a

x	NUN(NN)$_x$				NU(NN)$_x$			
	N–U–N	U--NN	N–N	ΔE	N–U	U--NN	N–N	ΔE
0	1117, 1.723		1.091		1037, 1.758		1.091	
1	1099, 1.729	2.826	1.091	−4.4	989, 1.757	2.357	1.127	−22.6
2	1081, 1.735	2.833	1.091	−4.5	966, 1.766	2.450	1.114	−7.8
3	1063, 1.740	2.818	1.091	−4.2	961, 1.767	2.493−2.550	1.105−1.109	−8.8
4	1042, 1.747	2.818	1.091	−3.7	966, 1.767	2.556	1.103	−7.9
5	1024, 1.753	2.811	1.091	−3.7	958, 1.766	2.574 avg	1.101−1.104	−3.0
6	1031, 1.750	2.932	1.091	+1.6	940, 1.768	2.634 avg	1.098−1.116	−3.4
7					922, 1.777	2.680 avg	1.098−1.103	+1.8

^{a}Energy changes (kcal/mol) for the addition of the next NN ligand to the nitride core or the previous complex. Gaussian basis sets are given in the SI for N and the SDD pseudopotentials for U. NUN and its complexes are singlet spin states, while UN and its complexes are quartet spin states ($\langle S^2 \rangle$ are between 3.78 and 3.75 before annihilation).
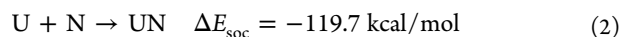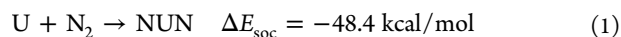
experiment. Note that the NUN(NN) band is stronger than the NUN band in the deposited sample and that only NU(NN)$_{1,2}$ bands are observed, now shifted to 971.4 and 963.6 cm⁻¹. Ultraviolet irradiation of the sample markedly increases the NUN(NN)$_{0,1,2,3,4,5}$ absorptions and destroys the NU(NN)$_{1,2}$ bands. Annealing cycles increase the terminal band for the NUN complexes until it dominates at 995.0 cm⁻¹. We attribute the shift from 1002.6 cm⁻¹ with 0.5% N$_2$ to 995.0 cm⁻¹ for 10% N$_2$ to the addition of a secondary ligand shell, which we denote as NUN(NN)$_5$(NN)$_y$. Annealing cycles form more UN with NN ligands, and only the terminal band is observed at 934.4 cm⁻¹, which shifts to 933.2, 932.4, and 931.7 cm⁻¹ on further annealing, while a new band appears at 879.8 cm⁻¹ and is denoted as NU(NN)$_6$(NN)$_y$. In pure nitrogen, the NN ligand saturated NUN band is very sharp at 995.7 cm⁻¹, and the saturated UN complex band is sharp at 878.2 cm⁻¹.

These absorptions are identified as NUN or UN species based on their 14/15 isotopic frequency ratios (Table 1), which are near 1.0309 for the antisymmetric N−U−N stretching mode of the linear molecule or near 1.0326 for the U−N diatomic vibration. In addition, the first member of the NUN progression at 1041.0 cm⁻¹ exhibits a 1/2/1 isotopic triplet with an intermediate ¹⁴N¹⁵N component at 1031.0 cm⁻¹ and a ¹⁵N¹⁵N counterpart at 1009.8 cm⁻¹ in spectra using the scrambled isotopic reagent mixture. This triplet pattern confirms that two equivalent N atoms are involved in the strong vibrational mode progression and shows the relationship to NUN itself. It is also possible to determine that the strongest first three members of the UN progression at 975.1, 965.9, and 957.1 cm⁻¹ *do not* have intermediate isotopic components, indicating that they are due to the vibration of a single N-atom-bearing species.

The above identifications were facilitated by DFT (B3LYP/SDD/6-311+G(3df) and G(2df,p)) frequency and energy calculations. It is straightforward to calculate NUN as a stable linear molecule in the $^1\Sigma_g^+$ ground state and to calculate its complexes with NN ligands; however, UN is more difficult to deal with because of its spin multiplicity. Higher level CASPT2 calculations revealed a $^4\Gamma$ ground-state UN molecule with a 1.757 Å bond length and harmonic frequency of 1034 cm⁻¹.[17] These calculations further showed that six valence electrons are located mostly in σ and degenerate π molecular orbitals. The three unpaired electrons are localized in 5f atomic orbitals on the U center. The UN molecule thus exhibits a 2.85 effective bond order.

A linear NU−NN species was explored next, but the calculated IR peaks were not in good agreement with experiment. Therefore, systematic PBE/def-TZVP calculations were performed on doublet and quartet states of NU−NN with bent, linear, and side-bonded structures, and the calculations showed that the bent quartet state had the lowest energy. To compute the vibrational modes, the B3LYP functional was used because it has been suggested for computing infrared spectra of uranium-containing species, and it has been used for similar compounds.[15,17−19] Table 2 lists the results of frequency calculations and dimensions for each singlet NUN and quartet UN complex. The table also shows the energy of formation for these complexes at the B3LYP level of theory with the SDD basis set on uranium and the corresponding ECP60MWP pseudopotential and the 6-311+G(2df,p) basis set for nitrogen.

The strong ¹⁴UN$_2$ band at 1050.9 cm⁻¹ is produced on direct insertion of laser-excited U atoms into dinitrogen, reaction 1, which is also carried further by full mercury arc (λ > 220 nm) irradiation but *not on stepwise sample warming (annealing).*[7] This reaction is 69.8 kcal/mol exothermic at the CASPT2 level in the absence of spin−orbit coupling (SOC) for ground-state U, which is reduced by 21.0 to 48.4 kcal/mol exothermic, including the effects of spin−orbit coupling for U using the RASSI method (see Supporting Information), but it requires the above ultraviolet energy excitation of U to activate the reaction. The sharp UN absorptions at 1001.1, 995.6, and 991.9 cm⁻¹ do increase slightly on annealing, which is probably due to the combination reaction 2. This is exothermic by 121.8 kcal/mol at the CASPT2 level without SOC correction, but it is reduced only slightly to 119.7 kcal/mol exothermic, including SOC for both U and UN. Nitrogen atoms are produced here by vacuum ultraviolet photolysis of N$_2$ with the laser-ablation plume: the production of N atoms is confirmed by observation of the N$_3$ radical in pure nitrogen experiments.[9,20]

$$U + N_2 \rightarrow NUN \quad \Delta E_{soc} = -48.4 \text{ kcal/mol} \tag{1}$$

$$U + N \rightarrow UN \quad \Delta E_{soc} = -119.7 \text{ kcal/mol} \tag{2}$$

The NUN and UN complexes with NN are produced spontaneously on annealing, as supported by exothermic addition reactions with computed energies that are given in Table 2. Structures for the saturated primary complexes are shown in Figure 3. There are several interesting differences between the two NN complex progressions. First, the binding of NN to quartet UN is much stronger than that for the closed shell NUN molecule, and the computed NU−NN distances are
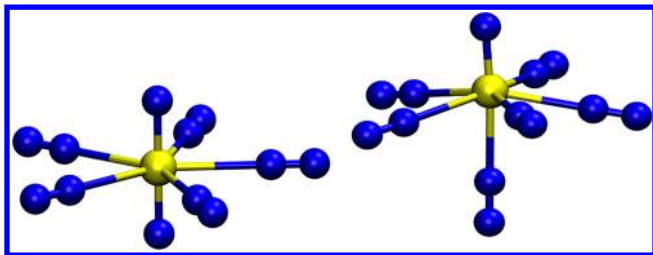
Figure 3. Structures of the stable $NUN(NN)_5$ and $NU(NN)_6$ complexes calculated at the B3LYP/SDD/6-311+G(2df,p) level.

clearly shorter than those for NUN−NN. Second, the complex progressions shifted 10 cm^{-1} below NUN but 25 cm^{-1} below the middle UN matrix site band, which attests to the stronger NN interaction with UN. The calculated frequencies in Table 2 follow this trend, but they overestimate the magnitude of the red shift. As noted above, there are only five bands in the NUN vibrational progression, but the UN progression contains six bands, as there is one additional site for ligation to UN. Note that the calculated U⋯NN distances increase substantially for the energetically unstable $NUN(NN)_6$ and $NU(NN)_7$ complexes that are *not* observed in the progressions. Finally, these matrix isolation and theoretical investigations of NUN and UN illustrate how readily these molecules bind even with the weak NN ligand, and this property might be extended to more synthetic work, which may involve weaker ligand systems.

■ CONCLUSIONS

The reactions of laser-ablated U atoms with N_2 molecules in excess argon during co-deposition at 4 K have produced intense NUN and weaker UN infrared absorptions. Sample annealing to allow diffusion of reagent species increased progressions of new absorptions identified as the $NUN(NN)_{1,2,3,4,5}$ and $NU(NN)_{1,2,3,4,5,6}$ uranium nitride complexes on the basis of nitrogen-15 isotopic substitution on the frequencies. Small matrix shifts are observed when the secondary coordination layers around the primary $NUN(NN)_{1,2,3,4,5}$ and NU-$(NN)_{1,2,3,4,5,6}$ complexes are changed from argon to nitrogen. Electronic structure and energy and frequency calculations provide support for the identification of these complexes and further characterization of the N≡U≡N and U≡N core molecules as terminal uranium nitrides with full triple bonds.

The uranium(III) molecule UN and its $UN(NN)_{1-6}$ complexes prepared in the argon matrix environment can be compared with the recently characterized multicyclic ligand-stabilized uranium(V) and (VI) terminal nitride complexes. First, the UN molecule has a CASPT2-computed 1.757 Å bond length and a 2.85 effective bond order, and the latter complexes have 1.825(15) and 1.799(7) Å terminal UN bond lengths and DFT computed 2.91 and 2.92 Mayer bond orders, respectively. This information characterizes terminal formal U≡N triple bonds.[17,4] The 996 cm^{-1} average matrix UN (III) site and the 955 and 914 cm^{-1} (V and VI) U−N stretching frequencies, respectively, are all in the U≡N triple bond region. These may be compared with the terminal triple bond in N≡UF$_3$, which has a CASPT2-calculated effective bond order of 2.78, a bond length of 1.759 Å, and an argon matrix stretching frequency of 938 cm^{-1}.[10] The observed matrix isolated UN diatomic isotopic U^{14}N/U^{15}N frequency ratio of 1.0326 is expected for this anharmonic diatomic oscillator, where the computed harmonic ratio is 1.0330.

However, isolated U≡N has a shorter CASPT2-calculated bond length of 1.757 Å and a higher computed frequency of 1034 cm^{-1} to go with the higher observed frequency of 996 cm^{-1} in solid argon. Significantly, the gas-phase UN bond distance has been measured as 1.7650(12) Å.[16] Notice that the observed U^{14}N/U^{15}N isotopic frequency ratio of 1.0326 for matrix-isolated UN is appropriate for an essentially pure anharmonic U−N bond stretching vibration, but the smaller 955/930 ratio of 1.0269 for the cyclic ligand (V) complex indicates considerable vibrational mode coupling with the ligand nitrogen centers. The 914/883 ratio of 1.0351 for the (VI) complex slightly exceeds the mechanical harmonic and anharmonic ratios, indicating some mode mixing in this larger terminal nitride system.

Although six-coordinating N_2 ligands reduce the U−N stretching frequency to 935 cm^{-1} in solid argon for the uranium(III) N≡U(NN)$_6$ complex, the terminal U≡N stretching mode is still a pure U−N mechanical vibration based on its 14/15 isotopic ratio, owing to the weak NN−UN ligand interaction. We computed the Mayer bond orders (MBO) for this series of dinitrogen complexes, and these results are compared in Table 3.[21,22] This approach is a

Table 3. Mayer Bond Orders (MBO) for UN, NN, $NU(NN)_x$, and $NUN(NN)_x$[a]

species	UN	U---NN	NN
UN	2.43	n/a	n/a
NN	n/a	n/a	3.27
UN(NN)	2.44	0.32	2.73
UN(NN)$_2$	2.39	0.19	2.81
UN(NN)$_3$	2.31	0.25	2.54
UN(NN)$_4$	2.29	0.13	2.61
UN(NN)$_5$	2.13	0.15	2.37
UN(NN)$_6$	2.01	0.28	1.82
NUN	2.15	n/a	n/a
NUN(NN)	2.17	0.08	3.23
NUN(NN)$_2$	2.16	0.10	3.01
NUN(NN)$_3$	2.12	0.10	2.79
NUN(NN)$_4$	2.06	0.10	2.56
NUN(NN)$_5$	2.01	0.11	2.26
NUN(NN)$_6$	1.95	0.07	2.54

[a]The average MBO value is given when more than one of that type of bond is present.

localization scheme based on the DFT electron density. In our earlier investigation of phosphide systems, we presented the CASPT2-calculated effective bond orders for UN and NUN as 2.85 and 2.87, respectively. Note that the Mayer bond orders based on the B3LYP electron density are smaller (2.43 and 2.15) and the 3.27 value for NN is higher than the textbook value; therefore, the values in Table 3 must be considered from these starting points. Note that, as expected from the observed frequencies and the computed bond lengths, the MBOs for the UN bonds decrease nicely in the NU(NN) and NUN(NN) complex series. Notice also that the MBO for NN in the first UN complex decreases much more than that for the first NUN complex, as shown by the decreases in computed frequency and the experimental observations.

The simple uranium−nitrogen triple bond was uncovered through matrix infrared spectroscopy and CASPT2 calculations in earlier publications on U≡N, N≡U≡N, and N≡UF$_3$ and

through comparison of U≡N with U≡P before the recent elegant synthetic work on UN ligand complexes.[4,6,7,10,17]

ASSOCIATED CONTENT

Ⓢ Supporting Information

Experimental and computational methods and references. Figure of matrix infrared spectra using 2.5% $^{14}N_2$ in argon. Cartesian coordinates for the title molecules. This material is available free of charge via the Internet at http://pubs.acs.org

AUTHOR INFORMATION

Corresponding Author
*E-mail: lsa@virginia.edu.

Notes
The authors declare no competing financial interest.

ACKNOWLEDGMENTS

REFERENCES

(1) (a) Hayton, T. W. *Chem. Commun.* **2013**, *49*, 2956−2973. (b) Burns, C. J. *Science* **2005**, *309*, 1823−1824. (c) Evans, W. J.; Kozimor, S. A.; Ziller, J. W. *Science* **2005**, *309*, 1835−1838.

(2) Hayton, T. W.; Boncella, J. M.; Scott, B. L.; Batista, E. R.; Hay, P. J. *Science* **2005**, *310*, 1941−1943.

(3) (a) Ephritikhine, M. *Dalton Trans.* **2006**, 2501−2516. (b) Cantat, T.; Arliguie, T.; Noel, A.; Thuery, P.; Ephritikhine, M.; Le Floch, P.; Mezailles, N. *J. Am. Chem. Soc.* **2009**, *131*, 963−972.

(4) (a) King, D. M.; Tuna, F.; McInnes, E. J. L.; McMaster, J.; Lewis, W.; Blake, A. J.; Liddle, S. T. *Science* **2012**, *337*, 717−720. (b) King, D. M.; Tuna, F.; McInnes, E. J. L.; McMaster, J.; Lewis, W.; Blake, A. J.; Liddle, S. T. *Nat. Chem.* **2013**, *5*, 482−488.

(5) Silva, G. W. C.; Yeamans, C. B.; Sattelberger, A. P.; Hartmann, T.; Cerefice, G. S.; Czerwinski, K. R. *Inorg. Chem.* **2009**, *48*, 10635−10642.

(6) Green, D. W.; Reedy, G. T. *J. Chem. Phys.* **1976**, *65*, 2921−2922.

(7) Hunt, R. D.; Yustein, J. T.; Andrews, L. *J. Chem. Phys.* **1993**, *98*, 6070−6074.

(8) Kushto, G. P.; Souter, P. F.; Andrews, L.; Neurock, M. *J. Chem. Phys.* **1997**, *106*, 5894−5903 (NUO, UN in solid argon).

(9) Kushto, G. P.; Souter, P. F.; Andrews, L. *J. Chem. Phys.* **1998**, *108*, 7121−7129 (UN_2 and UN in pure N_2).

(10) Andrews, L.; Wang, X.; Lindh, R.; Roos, B. O.; Marsden, C. J. *Angew. Chem., Int. Ed.* **2008**, *47*, 5366−5370.

(11) Wang, X.; Andrews, L.; Marsden, C. J. *Chem.—Eur. J.* **2008**, *14*, 9192−9201.

(12) Lyon, J. T.; Andrews, L.; Malmqvist, P.-Å.; Roos, B. O.; Yang, T.; Bursten, B. E. *Inorg. Chem.* **2007**, *46*, 4917−4925.

(13) Roos, B. O.; Lindh, R.; Cho, H.-G.; Andrews, L. *J. Phys. Chem. A* **2007**, *111*, 6420−6424 (CH_2=UH_2).

(14) Wang, X.; Andrews, L.; Malmqvist, P.-Å.; Roos, B. O.; Gonçalves, A. P.; Pereira, C. C. L.; Marçalo, J.; Godart, C.; Villeroy, B. *J. Am. Chem. Soc.* **2010**, *132*, 8484−8488 (UC, CUC)..

(15) Wang, X. F.; Andrews, L.; Vlaisavljevich, B.; Gagliardi, L. *Inorg. Chem.* **2011**, *50*, 3826−3831 (NUNH).

(16) Matthew, D. J.; Morse, M. D. *J. Chem. Phys.* **2013**, *138*, 184303.

(17) Vlaisavljevich, B.; Gagliardi, L.; Wang, X. F.; Liang, B.; Andrews, L. *Inorg. Chem.* **2010**, *49*, 9230−9235 and references therein.

(18) Van Stipdonk, G. S.; de Jong, W. A.; Oomens, J.; Gresham, G. L.; McIlwain, M. E.; Gao, D.; Siboulet, B.; Visscher, L.; Kullman, M.; Polfer, N. *ChemPhysChem* **2008**, *9*, 1278−1285.

(19) Wang, X. F.; Andrews, L.; Ma, D.; Gagliardi, L.; Gonçalves, A. P.; Pereira, C. C. L.; Marçalo, J.; Godart, C.; Villeroy, B. *J. Chem. Phys.* **2011**, *134*, 244313.

(20) Tain, R.; Facelli, J. C.; Michl, J. *J. Phys. Chem.* **1988**, *97*, 4073−4076.

(21) Mayer, I. *Chem. Phys. Lett.* **1983**, *97*, 270−274.

(22) Bridgeman, A. J.; Cavigliasso, G.; Ireland, L. R.; Rothery, J. *J. Chem. Soc., Dalton Trans.* **2001**, 2095−2108.